In-situ CO_2 sequestration and nutrients removal in an anaerobic digestion-microbial electrolysis cell by silicates application: Effect of dosage and biogas circulation

Yan Zhang[a,b,c], Linlin Gong[a], Qianqian Jiang[a], Min-Hua Cui[a,b,c], Jie Zhang[a], He Liu[a,b,c,*]

[a] School of Environment and Civil Engineering, Jiangnan University, Wuxi 214122, China
[b] Jiangsu Key Laboratory of Anaerobic Biotechnology, Wuxi 214122, China
[c] Jiangsu Collaborative Innovation Center of Water Treatment Technology and Material, Suzhou 215011, China

HIGHLIGHTS

- CO_2 capture and nutrients removal were achieved in AD-MEC by silicate addition.
- 47.4% NH_4^+ and 92.1% PO_4^{3-} were simultaneously removed by silicate addition.
- Biogas circulation enhanced CH_4 production from 164.8 mL/g COD to 261.5 mL/g COD.
- CH_4 content reached 96.7% with mineral CO_2 sequestration and biogas circulation.

GRAPHICAL ABSTRACT
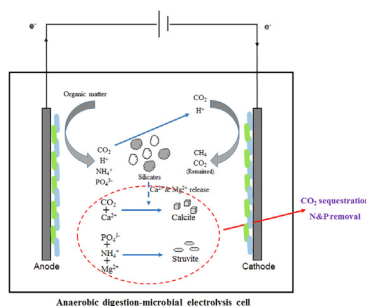
ABSTRACT

For overcoming high CO_2 content in biogas and high NH_4^+ and PO_4^{3-} concentrations in digestate of anaerobic digestion - microbial electrolysis cell (AD-MEC), in-situ CO_2 sequestration and nutrients removal were investigated in AD-MEC by combined application of wollastonite and magnesium silicate. Wollastonite of 20 g/L and magnesium silicate of 40 g/L was the optimal dosage for CO_2 sequestration and nutrients removal in the AD-MEC, which decreased CO_2 content from 11.5% to 7.8%, and removed NH_4^+ and PO_4^{3-} by 47.4% and 92.1%, respectively, by forming calcite and struvite precipitates. Higher silicates dosage enhanced little in CO_2 sequestration and nutrients removal probably owing to the limitation of proton inventory for Ca^{2+} and Mg^{2+} release. Biogas circulation slightly deteriorated mineral CO_2 sequestration and nutrients removal in AD-MEC, but enhanced CH_4 production from 164.8 mL CH_4/g CODr to 261.5 ± 5.1 mL CH_4/g CODr. Integrating biogas circulation with silicates application in AD-MEC resulted in the CH_4 content reached 96.7% ± 0.4%. High-throughput sequencing revealed that *Geobacter* was the dominant bacterial genus, while hydrogenotrophic methanogens of *Methanobacterium* and *Methanomassiliicoccus* dominated in archaeal communities on both anode and cathode in the AD-MEC with silicates addition. In conclusion, the combined application of wollastonite and magnesium silicate is an attractive way to improve the performance of AD-MEC by achieving in-situ mineral CO_2 sequestration and nutrients removal.

* Corresponding author at: School of Environment and Civil Engineering, Jiangnan University, Wuxi 214122, China.
  E-mail address: liuhe@jiangnan.edu.cn (H. Liu).

1. Introduction

The treatment of wastewater and sewage sludge has been identified as a contributor to anthropogenic greenhouse gas (GHG) emission [1,2]. Reducing CO_2 emission from wastewater treatment plants (WWTPs) is an important active contribution to climate change mitigation [3,4]. For decreasing CO_2 emission and achieving carbon neutral WWTPs, anaerobic digestion (AD) has been extensively recommended for the treatment of organic wastewater and excessive sludge in WWTPs [5,6]. However, slow conversion of organic matter in AD process and relatively low CH_4 content in the produced biogas [7–9] decreased energy recovery and carbon emission reduction efficiency. Currently, studies have developed AD - microbial electrolysis cell (MEC) system to overcome the shortages of AD. By applying an external voltage, AD-MEC accelerated substrate degradation, enhanced CH_4 production, and increased CH_4 content in biogas, compared to conventional AD process [8–10]. However, CO_2 with content higher than 10% is usually remained [11–13], which restricts the direct utilization of AD-MEC produced biogas. Additional biogas upgrading process increases biogas production cost by 20–72% [14] and may cause a methane loss of 0.1–8% [15], which increases carbon emission. Developing in situ CO_2 sequestration in AD-MEC is an attractive way for biogas upgrading, and thus enhancing CO_2 emission reduction of WWTPs with AD-MEC application.

Mineral CO_2 sequestration is a process where CO_2 is fixed in the form of carbonates based on alkaline silicates (as shown in Equation (1)) [16,17].

$$(\text{Mg, Ca})_x\text{Si}_y\text{O}_{x+2y+z}\text{H}_{2z(s)} + x\text{CO}_{2(g)}$$
$$\rightarrow x(\text{Mg, Ca})\text{CO}_{3(s)} + y\text{SiO}_{2(s)} + z\text{H}_2\text{O} \qquad (1)$$
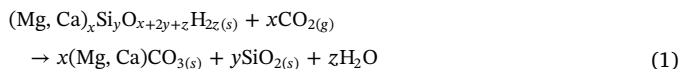
This process consists of two steps: (1) the release of cations and (2) the formation of carbonate precipitates. Since acidic and alkaline conditions are respectively conducive to the release of cations and the formation of carbonate precipitates, mineral CO_2 sequestration could be coupled in biotechnological processes that involve a sequence of an acid-producing and an alkalinity-producing step [17]. Several previous studies have applied mineral CO_2 sequestration in AD process, which combined a VFAs producing stage and a methane producing stage [14,18,19]. Integrating MEC in AD, AD-MEC has a bio-anode oxidizing organic matters with proton generation, and a bio-cathode reducing CO_2 to CH_4 with an alkaline increase, which is more conducive to couple the two steps of mineral CO_2 sequestration. Therefore, mineral CO_2 sequestration could be adopted as a potential in-situ CO_2 sequestration technology for AD-MEC.

In addition, the removal of the high concentration of PO_4^{3-} and NH_4^+ from digestate liquid is another tough problem along with the AD-MEC process. Application of silicates in AD-MEC also provides an opportunity to remove PO_4^{3-} and NH_4^+ simultaneously with mineral CO_2 sequestration. The Ca^{2+} and Mg^{2+} released from the silicates can react with phosphate and ammonium to form precipitates, thereby reducing the nutrients concentration in the digestate liquid. A previous study has found that the Ca^{2+}/Mg^{2+} ratio significantly affects the composition of the formed precipitates and further influences CO_2 sequestration and nutrients removal, and equal molar of Ca^{2+} and Mg^{2+} released from the silicates is the key parameter for good performance of simultaneous CO_2 sequestration and nutrients removal in AD system [18]. This indicates that in AD-MEC, simultaneous CO_2 sequestration and nutrients removal may also achieved by addition of silicates with suitable composition. The Ca^{2+}/Mg^{2+} ratio suggested in the previous study based on AD process could be adopted in AD-MEC, however, the dosage of the silicates needs to be optimized. In addition, after CO_2 sequestration by silicates in AD, CO_2 remained in biogas with content of 18.99%, and Ca^{2+} and Mg^{2+} remained in the liquid with concentration of 79.3 mg/L and 60.7 mg/L, respectively, which indicated that the cations were not fully utilized. It is necessary to develop measures to

improve the utilization of cations and enhance CO_2 sequestration. Biogas circulation can enhance the contact between the residual CO_2 and the cations, thus is a potential measure to improve mineral CO_2 sequestration. However, the actual impact of biogas circulation on mineral CO_2 sequestration has not been reported. Therefore, this study aims to (1) apply silicates in AD-MEC to verify the feasibility of silicates mediated CO_2 and nutrients sequestration in AD-MEC, (2) optimize the dosage of silicates to achieve the best performance of mineral CO_2 and nutrients sequestration, (3) investigate the effect of biogas circulation on mineral CO_2 and nutrients sequestration in AD-MEC with silicates addition. This is the first study on mineral CO_2 and nutrients sequestration in AD-MEC. The microbial community in the AD-MEC coupled with mineral CO_2 sequestration and nutrients removal was also analyzed.

2. Materials and methods

2.1. MEC setup

The reactor used in this study was a cylinder single-chamber MEC made of plexiglass (shown in Fig. S1). The volume of the MEC was approximate 500 mL, with a diameter of 8 cm and a height of 10 cm. A carbon fiber brush with a diameter of 6 cm and a length of 8 cm was fixed in the center of the reactor and used as the anode. The cathode was a 200-mesh nickel screen with a length of 25.5 cm and a width of 10 cm, which was fixed on the inner wall of the cylinder reactor. A DC power supply (3465A, Array, Nanjing) was used to apply a voltage of 0.8 V across the anode and cathode. A Ag/AgCl electrode (Model 218, Rex, Shanghai) was fixed on the top of the reactor as the reference electrode. A 10 Ω resistor was connected between the anode and cathode for calculating the current in the circuit. A data acquisition system (2700, Keithley, USA) was used to collect the electrochemical data. The liquid in the AD-MEC was stirred with a magnetic stirrer during operation. The generated biogas was collected with a gas bag installed on the top of the reactor. During silicate addition periods, the silicates were filled in a 3500 D dialysis bag, and fixed around the anode with nylon thread.

2.2. Inoculum, substrate, and silicates

Secondary effluent of a local WWTP was adopted as the inoculum of the AD-MEC. The substrate used was the hydrolysate of the excess sludge collected from the same WWTP. The sludge, with total solids (TS) of 136.0 ± 1.0 g/L and the ratio of volatile solids (VS) to TS of 53.7% ± 0.9%, was firstly diluted to TS of 60 g/L. Subsequently, the diluted sludge was thermally treated for 24 h at 90 °C. The sludge hydrolysate was obtained by centrifuging at 8000 rpm for 10 min. Before use, the supernatant, i.e. sludge hydrolysate, was diluted to approximate 2200 mg-COD/L with deionized water. The silicates used in this study were the same as previously reported [18]. In brief, calcium silicate used was wollastonite, which was grinded and screened with 120 mesh; magnesium silicate used was in analytical reagent (AR) grade purchased from Sinopharm Chemical Reagent Co., Ltd.

2.3. Reactor operation

The AD-MEC was started up with sodium acetate as the substrate for rapid enrichment of electrode biofilm. The substrate of the reactor was gradually changed from the acetate solution to the sludge hydrolysate. The AD-MEC was finally stably operated in batch mode under the hydraulic retention time (HRT) of 3 days per batch with sludge hydrolysate as the substrate. The details of the operation during starting up are shown in the Supplementary materials (Text S1). After the AD-MEC was stably operated, silicates were added into the reactor. According to a previous study [18], equimolar Mg^{2+} and Ca^{2+} released from silicates is the key parameter for simultaneous mineral CO_2 and nutrients
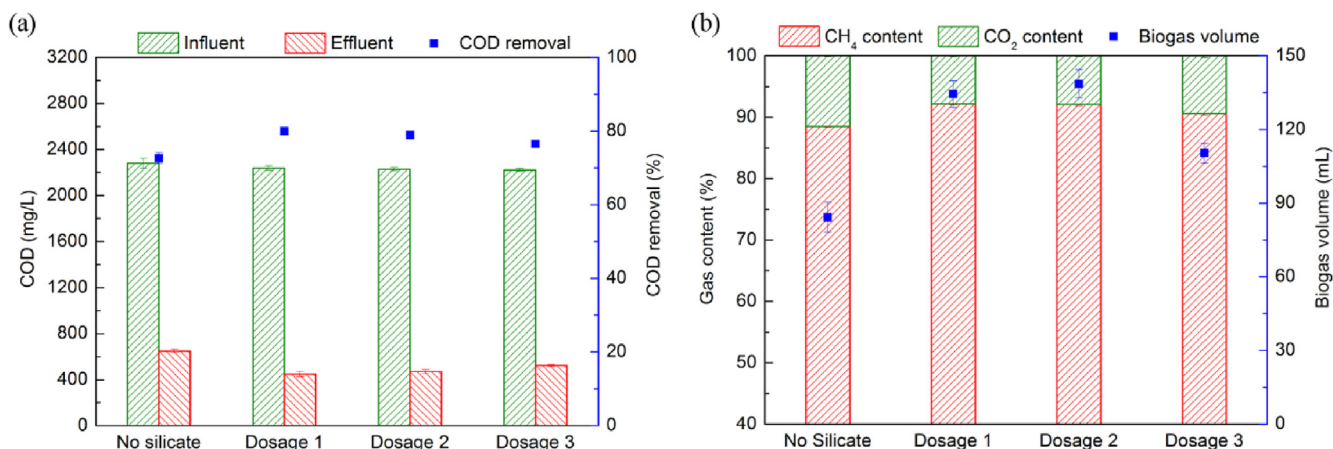
Fig. 1. COD removal and biogas production of the AD-MEC under different silicate dosages. (a) COD removal, (b) biogas production. Error bars represent the standard deviations of the four replicate batches under each silicate dosage.

sequestration. In addition, wollastonite and magnesium silicate with weight ratio of 2:1 could release almost equimolar Mg^{2+} and Ca^{2+} in weak acid condition [18]. Therefore, wollastonite and magnesium silicate with weight ratio of 2:1 were applied in this study for simultaneous CO_2 sequestration and nutrients removal. For optimizing the silicate dosage, three dosages of 40 g/L wollastonite and 20 g/L magnesium silicate (dosage 1), 80 g/L wollastonite and 40 g/L magnesium silicate (dosage 2), and 20 g/L wollastonite and 10 g/L magnesium silicate (dosage 3) were successively applied, and the performance under the three dosages were compared. After optimizing silicate dosage, the impact of biogas circulation on the performance of the AD-MEC without and with silicate addition was investigated. Four batches were conducted under each operation condition. The effective volume of hydrolysate treated per batch was controlled at 420 mL without silicates addition and 400 mL during silicates addition. At the end of each batch, all the treated hydrolysates were discharged and replaced with new hydrolysates for the next batch, and the used silicates were taken out and replaced with new minerals if it was in silicates addition stages. After hydrolysate loading, N_2 gas was purged into the reactor at a rate of 0.5 L/min for 10 min to eliminate residual oxygen. The precipitates in the effluent of each batch were recovered by centrifugation at 8000 rpm for 5 min. All the precipitates recovered from the four batches of each operation condition were mixed, and further analyzed by scanning electron microscope (SEM) and X-ray diffraction (XRD). For biogas circulation, the biogas collected in the gas bag was circulated into the bottom of the AD-MEC with a peristaltic pump under a flux of 60 mL/h, which was started at 12 h after the start of each batch. All the operation of the AD-MEC was under 35 °C.

2.4. Analytical methods

The parameters of pH, COD, NH_4^+-N, and PO_4^{3-}-P were determined according to standard methods [20]. Biogas component was analyzed by a gas chromatography (GC9790II, FULI, China) installed with a carbon molecular sieve packed stainless steel column (TDX-01, inner diameter 3 mm, length 2 m) and a thermal conductivity detector (TCD). The biogas volume was measured by displacement of saturated NaCl solution in a graduated measuring cylinder [21]. The concentrations of Ca^{2+} and Mg^{2+} were measured with an AA-7700 atomic absorption spectrophotometer (Shimadzu, Japan). The SEM analysis was conducted based on a EVO18 (ZEISS, Germany), and the XRD analysis was carried out using a D8 Advance DMAX2RB (Bruker, Germany).

2.5. Microbial community analysis

A piece of anode and cathode with biofilm were cut from the reactor

after the experiment operation. The morphology of the biofilm on cathode was observed based on SEM to investigate whether there would be precipitates attached. The DNA of the biofilms on both pieces from anode and cathode were extracted using the DNA PowerSoil® Total DNA Isolation Kit (Mo Bio, Carlsbad, CA). The concentration of extracted DNA was detected with a UV–Vis spectrophotometer (NanoDrop 2000, Thermo Fisher, MA). High-throughput sequencing was conducted in Majorbio Biomedical Technology Co., Ltd. based on Illumina Miseq PE300, with primers of 338F (5′-ACTCCTACGGGAGGCAGCAG -3′) and 806R (5′-GGACTACHVGGGTWTCTAAT-3′) for bacterial 16S rRNA, and 524F10extF (5′-TGYCAGCCGCCGCGGTAA-3′) and Arch958RmodR (5′-YCCGGCGTTGAVTCCAATT-3′) for archaeal 16S rRNA. First, the PCRs of target genes were conducted on a GeneAMP® 9700 (ABI, USA) with a TransStart Fastpfu DNA Polymerse (AP221-02, TransGen, China) in triplicate. The mixture of the triplicate PCR products was purified with 2% agarose gel electrophoresis and a DNA gel extraction kit (AxyPre, Axygen, USA). The purified amplicons were quantified by a QuantiFluor^{TM}-ST (Promega, USA), drawn in equimolar, and paired-end sequenced. The sequencing data were processed with QIIME as previously described [22]. The operational taxonomic units (OTUs) were assembled with a 97% similarity cutoff using Usearch [23]. The taxonomy was assigned by comparing to the SILVA database [24] with RDP Classifier [25]. The raw reads were deposited into the NCBI Sequence Read Archive (SRA) database (Accession Number: PRJNA576720).

2.6. Statistical analysis method

Significance was analyzed with ANOVA based on Student – Newman – Keulstest method using SPSS 17.0.

3. Results and discussion

3.1. Performance of AD-MEC under different silicate dosage

The COD removal and biogas production of the AD-MEC treating sludge hydrolysate under different silicate dosages are shown in Fig. 1. The COD of the influent sludge hydrolysate was 2241.8 ± 33.1 mg/L, which was decreased to 624.0 ± 23.3.1 mg/L with the treatment of AD-MEC with no silicate addition (Fig. 1a). The AD-MEC achieved good COD removal of 72.6% ± 1.5% under HRT of 3 days, which was much higher than the COD removal (44.92%) of reported AD-MEC treating similar sludge hydrolysate [26]. With silicates addition, the COD removal was significantly increased (α = 0.01), and reached 80.0% ± 0.8%, 78.9% ± 0.8%, and 76.5% ± 0.3% under dosage 1, dosage 2, and dosage 3, respectively. In which, the COD removal under

dosage 1 and dosage 2 was significantly higher than that under dosage 3, however, no significant difference was indicated between that under dosage 1 and dosage 2 based on ANOVA at $\alpha = 0.01$. In general, the addition of the silicates promoted the degradation of organic matters in the AD-MEC.

In accordance with the promotion of COD removal, the addition of the silicates also enhanced biogas production (Fig. 1b). Without silicates addition, the biogas yield of the AD-MEC was 84.3 ± 6.1 mL per batch, with a CH_4 yield of 74.6 ± 5.4 mL per batch. With silicates addition under dosage 1 and dosage 2, the CH_4 yield was increased to 123.8 ± 5.1 mL per batch and 127.5 ± 5.4 mL per batch, respectively. Under dosage 3, the biogas production was also improved, however, the CH_4 yield was only 100.0 ± 3.9 mL per batch, significantly less than that under dosage 1 and dosage 2 ($\alpha = 0.01$). The addition of the silicates also improved the CH_4 production of the AD-MEC, which was 164.8 ± 7.9 mL CH_4 per gram COD removed (mL CH_4/g CODr), 172 ± 5.1 mL CH_4/g CODr, and 140.2 ± 6.0 mL CH_4/g CODr, respectively, under dosage 1, dosage 2 and dosage 3, much higher than that without silicates addition (107.4 ± 9.9 mL CH_4/g CODr). There was no significant difference in CH_4 production under dosage 1 and dosage 2, but both were significantly higher than dosage 3. Meanwhile, CH_4 content in the produced biogas was increased with silicates addition. Under dosage 1, dosage 2 and dosage 3, the CH_4 content was $92.2\% \pm 0.2\%$, $92.1\% \pm 0.2\%$, and $90.6\% \pm 0.3\%$, respectively, which was significantly higher than that without silicates addition ($88.5\% \pm 0.1\%$).

The changes of NH_4^+-N and PO_4^{3-}-P concentrations in the AD-MEC under different dosages are shown in Fig. 2. Without silicates addition, NH_4^+-N concentration increased from 23.2 ± 3.2 mg/L before treatment to 125.7 ± 4.2 mg/L after treatment due to the degradation of organic matter. With a combined addition of wollastonite and magnesium silicate, the NH_4^+-N concentration in the hydrolysate after treatment showed a significant decline. Under the lowest dosage, dosage 3, NH_4^+-N concentration of effluent reduced to 101.4 ± 3.0 mg/L, 19.3% less than that during no silicates addition. With higher dosages of dosage 1 and dosage 2, the effluent NH_4^+-N concentration further decreased to 66.1 ± 1.5 mg/L and 71.6 ± 2.7 mg/L, respectively, which was 47.4% and 43.0% lower than that without silicates. The phosphate removal performance with silicates addition was even better than that of ammonia removal. In the period without silicates addition, the PO_4^{3-}-P concentration in the effluent was 67.2 ± 2.1 mg/L, which was decreased to 39.1 ± 1.8 mg/L with silicates addition under dosage 3. Under the higher dosage of dosage 1 and dosage 2, the effluent PO_4^{3-}-P concentration decreased to 5.3 ± 1.3 mg/L and

3.9 ± 1.1 mg/L, which was 92.1% and 94.1% lower than that without silicates addition, respectively.

According to the decrease of CO_2 content in biogas and the declined nutrients concentration in effluent, it indicated that the combined application of wollastonite and magnesium silicate achieved in-situ CO_2 sequestration and nutrients removal in the AD-MEC. Comparing that under different dosages, it could be found that the low dosage, dosage 3, which was 20 g/L wollastonite and 10 g/L magnesium silicate, achieved the worst performance in both CO_2 sequestration and nutrients removal. Under medium dosage of 40 g/L wollastonite and 20 g/L magnesium silicate (dosage 2), the CO_2 sequestration and nutrients removal were significantly improved, of which CH_4 content increased to 92.1%, and PO_4^{3-}-P concentration in the effluent was only 5.3 ± 1.3 mg/L. However, further increasing dosage achieved a limited improvement of CO_2 sequestration and nutrients removal. Therefore, 40 g/L wollastonite and 20 g/L magnesium silicate, was the optimal dosage for in-situ CO_2 sequestration and nutrients removal in the AD-MEC.

The mineral CO_2 sequestration and nutrients removal inevitably accompanied by pH and cation concentration changes. The change of pH in AD-MEC under different silicate dosages are shown in Fig. S2. The initial pH in the AD-MEC was controlled at 7.10–7.16. Without silicates addition, the pH of the treated hydrolysate was 7.45 ± 0.02, higher than that before treatment. The silicates addition significantly improved the effluent pH. In the case of dosage 1, dosage 2, and dosage 3, the effluent pH increased to 8.14 ± 0.02, 8.20 ± 0.01, and 8.00 ± 0.04, respectively. The increase of pH in the AD-MEC with silicate addition was consistent with that in the silicate added AD system [18,19]. This is due to the consumption of proton during the first step of mineral CO_2 sequestration, i.e. silicate dissolution and cations release [17,27]. Consistently, as shown in Fig. 3, the Ca^{2+} and Mg^{2+} in the AD-MEC increased rapidly in the first day of each batch with silicates addition, which was due to silicate dissolution and the release of cations with proton consumption. During the subsequent operation in each batch, the Ca^{2+} and Mg^{2+} concentrations decreased rapidly owing to the enhanced precipitation reactions with the rise of pH. Since the samples were taken at 24 h intervals, it was not possible to determine whether there was a higher concentration before or after 24 h than that at 24 h. However, the data has already shown the trend of cation concentrations increased first and then decreased, and supported the achievement of mineral CO_2 and nutrients sequestration. In the period without silicate addition, the concentration of Ca^{2+} increased slightly. Considering the sludge itself contains a certain amount of calcium elements [28], the increase of Ca^{2+} concentration in the
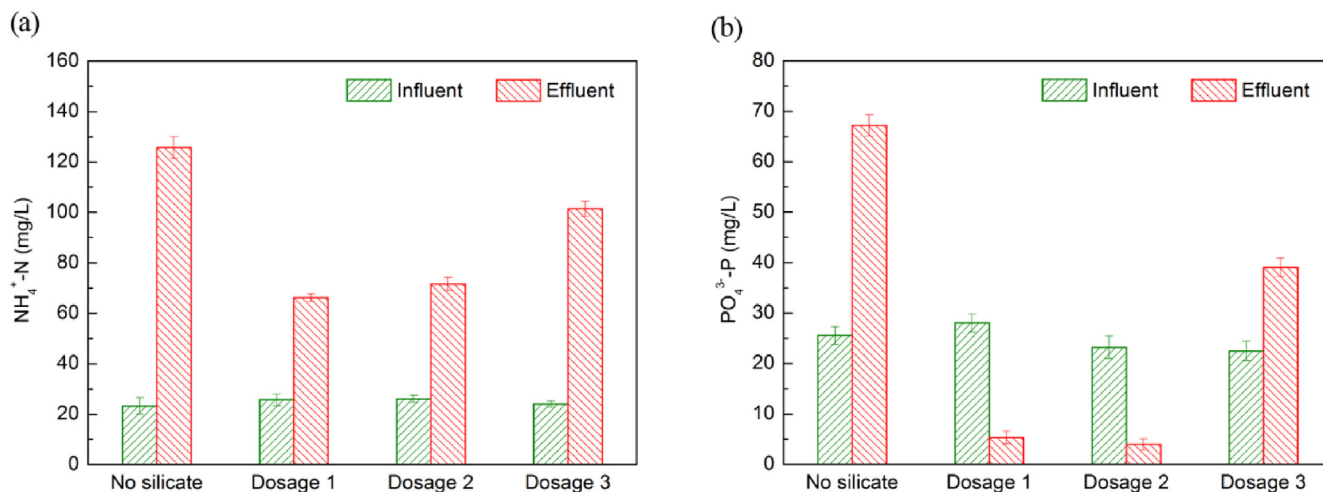

Fig. 2. NH_4^+-N and PO_4^{3-}-P concentrations in the AD-MEC under different silicate dosages. (a) NH_4^+-N, (b) PO_4^{3-}-P. Error bars represent the standard deviations of the four replicate batches under each silicate dosage.
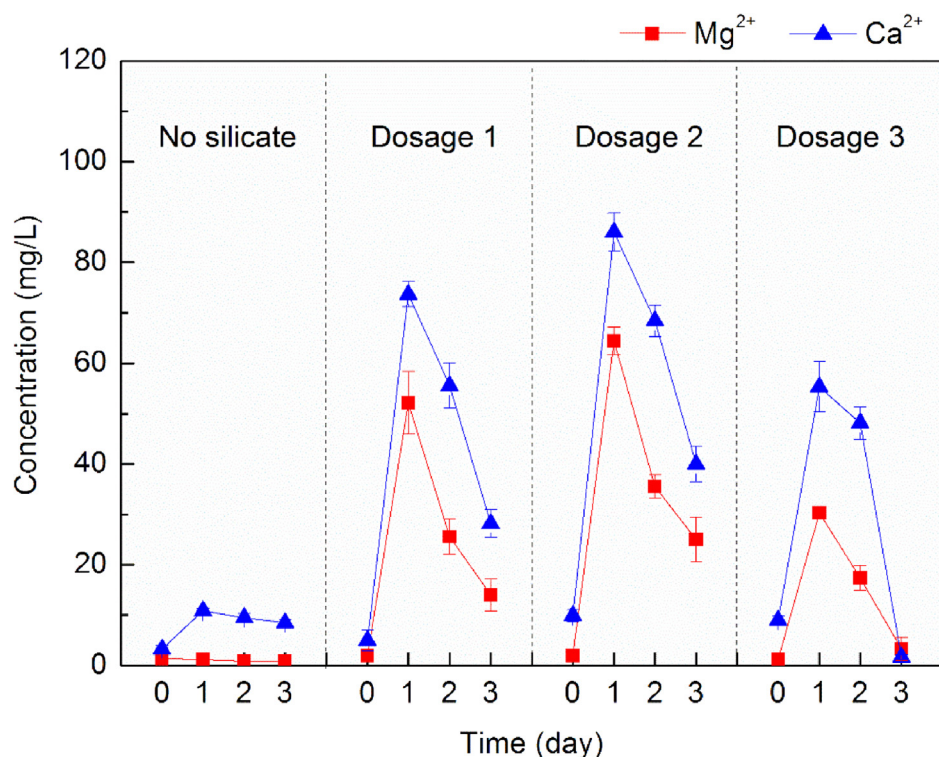
Fig. 3. Variation of Ca^{2+} and Mg^{2+} concentrations during AD-MEC operation under different silicate dosages. Error bars represent the standard deviations of the four replicate batches under each silicate dosage.

period without silicate addition might be caused by the release of Ca^{2+} from residual colloids in the sludge hydrolysate.

Compare the Ca^{2+} and Mg^{2+} concentration under the three different dosages, it could find that the Ca^{2+} and Mg^{2+} concentration at the end of each batch under dosage 3 was closed to zero, which means that most of the Ca^{2+} and Mg^{2+} was precipitated, and indicated the dosage was insufficient. The insufficient cation under dosage 3 resulted in the relatively poor performance of CO_2 sequestration and nutrients removal (Fig. 1 and Fig. 2). For the two increased dosages, dosage 2 was the double of dosage 1, however, the concentration of Ca^{2+} and Mg^{2+} during operation under dosage 2 was only slightly higher than that under dosage 1. The reasons might be: (1) the highest concentration of Ca^{2+} and Mg^{2+} was not detected owing to the sampling intervals; (2) the Ca^{2+} and Mg^{2+} may be consumed by precipitation simultaneously with the dissolution of silicates, owing to the higher pH near the cathode than that of bulk liquid in the AD-MEC. In addition, the release of cations is restricted by the amount of available protons. If the amount of protons becomes a limit, the amount of released cations will not increase significantly even if the silicate dosage is increased. In this study, the increase of Ca^{2+} and Mg^{2+} concentrations were less when the dosage increased from dosage 1 to dosage 2 (relatively high dosage) than that when the dosage increased from dosage 3 to dosage 1 (relatively low dosage). It indicated that the amount of protons might have been a restrictive factor for silicates dissolution under the high dosage of dosage 2. In addition, different from that under dosage 3, Ca^{2+} and Mg^{2+} remained at the end of each batch under dosage 1 and dosage 2, which indicated that the cations released from the silicates might be sufficient for CO_2 sequestration and nutrients removal under dosage 1 and dosage 2. This also answered why similar CO_2 sequestration and nutrients removal performance achieved under doubled silicate dosage (dosage 2) compared to dosage 1.

With mineral CO_2 sequestration and nutrients removal, precipitates generated in the AD-MEC with silicates addition. The generated precipitates were basically discharged out of the reactor with the liquid after each batch, however, a very small amount of the precipitates

inevitably remained inside the reactor. In addition, the precipitates collected by centrifugation were accompanied by a small amount of flocs that might be detached from the biofilm. Therefore, a quantitative analysis of the precipitates was not conducted. However, the morphology and the components of the precipitates were analyzed with SEM and XRD (shown in Fig. S3). As shown in the SEM photos, the generated precipitates under the three dosage were basically the same, mainly composed of two types of particles, i.e. small square particles and long strips with slightly larger individual sizes. The XRD pattern of the precipitates was consistent with the mixed standard pattern of Calcite (PDF#05-0586) and Struvite (PDF#71-2089). Based on SEM and XRD, it can be concluded that the precipitates were mainly composed of calcite ($CaCO_3$) and struvite ($MgNH_4PO_4$). The pH of bulk liquid at the end of each batch with silicates addition in this study was 8.00–8.20, which is not the best pH for struvite formation. However, a previous study has proved the formation of struvite under slightly alkaline environment of pH around 8.0 [18]. In addition, due to the consumption of protons at cathode in the AD-MEC, the pH near the cathode should be higher than that of bulk liquid and beneficial to the formation of struvite. With calcite and struvite formation, CO_2 sequestration and nutrients removal were achieved in the AD-MEC.

The ratio of wollastonite to magnesium silicate significantly affects the performance of CO_2 sequestration and nutrients removal [18]. The number of protons required for Ca^{2+} and Mg^{2+} release from calcium silicate and magnesium silicate is the same, which means that the total amount of Ca^{2+} and Mg^{2+} released from the silicates is basically the same in the same AD-MEC. The silicates with a high proportion of calcium silicate will increase the concentration of dissolved Ca^{2+} overwhelming Mg^{2+}, thus forming calcium carbonate and calcium phosphate, weakening the removal of NH_4^+. The addition of high magnesium silicate proportion leads to more dissolved Mg^{2+}, which is conducive to the generation of $MgNH_4PO_4$ and remove NH_4^+ and PO_4^{3-}, however, the CO_2 sequestration will be deteriorated due to the weaker CO_2 sequestration ability of Mg^{2+} than that of Ca^{2+} [18]. The proportion of silicates added in this study was determined according to

the previous study [18]. The ratio of wollastonite to magnesium silicate at 2:1 could release nearly equal molar of Ca^{2+} and Mg^{2+} in weak acid, which is conducive to achieving the best performance of CO_2 sequestration and nutrients removal [18]. Natural wollastonite may contain a small amount of Fe and Mn, which may result in the generation of other precipitates such as $Fe(OH)_3$, $Mn(OH)_2$, $FePO_4$, and $MnPO_4$. However, due to the low content, Fe and Mn in the silicates will hardly affect the operation of this process. The wollastonite used in this study was the natural mineral, and no substances other than calcite and struvite were detected in the precipitates. The results indicated the negligible impact of impurities in wollastonite on mineral CO_2 and nutrients sequestration in AD-MEC.

CH_4 production of the AD-MEC was also increased with silicates addition. As alkaline pH benefits the hydrolysis of organic matter [29,30], the increased pH in the AD-MEC with silicates addition (Fig. S2) should be one of the potential reasons for CH_4 production enhancement. The increased Ca^{2+} and Mg^{2+} might be another reason for the improvement of CH_4 production. In previous studies, the biogas yield of AD was improved up to 30% with moderate Ca^{2+} or Mg^{2+} addition (less than 1000 mg/L) [31,32], though a negative impact on CH_4 production was found at higher Ca^{2+} or Mg^{2+} concentration [31–33]. In this study, the highest Ca^{2+} and Mg^{2+} concentrations were 61.0–89.4 mg/L, which fitted in the moderate concentration range that might stimulate the CH_4 production. In addition, the release of Ca^{2+} and Mg^{2+} increased the conductivity of the solution, promoted electron transfer, which was conducive to the improvement of AD-MEC performance. CO_2 sequestration and nutrients removal, accompanied by CH_4 production enhancement make silicates application in AD-MEC very attractive.

3.2. Effect of biogas circulation on the performance of AD-MEC with silicates addition

Under high silicates dosages of dosage 1 and 2, there were Ca^{2+} and Mg^{2+} remained at the end of each batch. Considering the PO_4^{3-} was rarely remained, it is hard to improve cations utilization by enhancing struvite precipitation. However, CO_2 with 10% content remained in the biogas. Therefore, biogas circulation was applied to the AD-MEC in order to enhance the contact of CO_2 with the cations, which may probably enhance the utilization of the cations. The impact of biogas circulation on CO_2 sequestration and nutrients removal was further investigated.

The COD removal and biogas production performance of the AD-MEC with biogas circulation are shown in Fig. 4. Without silicates addition, the COD removal of the AD-MEC with biogas circulation was 72.5% ± 1.4%, which was generally consistent with that without biogas circulation. However, CH_4 production was significantly increased from 107.4 ± 9.9 mL CH_4/g CODr to 208.4 ± 5.1 mL CH_4/g CODr, with CH_4 content increased from 88.5% ± 0.1% to 93.6% ± 0.3%, by biogas circulation application. Consistent with that in normal AD-MEC, silicates addition improved the COD removal in the AD-MEC with biogas circulation (Fig. 4a). In AD-MEC with biogas circulation and silicates addition, the COD removal was 80.3% ± 0.9%, which was basically the same with that of AD-MEC without biogas circulation but with silicates addition (80.0% ± 0.8%). Silicates addition promoted the degradation of both proteins and polysaccharides in the AD-MEC (Fig. S4). Although the COD removal was similar, the CH_4 production of the silicates added AD-MEC reached 261.5 ± 5.1 mL CH_4/g CODr with biogas circulation, which was significantly higher than that of silicates added AD-MEC without biogas circulation (164.8 ± 7.9 mL CH_4/g CODr). The improvement of COD removal and CH_4 production by silicate addition was similar between that with and without biogas circulation. With CH_4 production and CH_4 content improvement by applying biogas circulation in silicates added AD-MEC, the CO_2 content was further decreased with CH_4 content reached 96.7% ± 0.4%, which met the CH_4 content requirement (96%) of pipeline biomethane [34].

Silicates also remarkably reduced NH_4^+ and PO_4^{3-} concentration in the AD-MEC with biogas circulation (Fig. 5). At the end of each batch, the NH_4^+-N and PO_4^{3-}-P concentrations were 83.8 ± 0.4 mg/L and 6.2 ± 0.5 mg/L, respectively, and 34.2% and 90.7% lower than that with no silicates addition. In the AD-MEC with biogas circulation, silicates addition also significantly increased the pH (Fig. S5), with the Ca^{2+} and Mg^{2+} concentration presented an increase–decrease curve (Fig. S6). With silicates addition, fine precipitates also formed in the AD-MEC with biogas circulation, which was consistent with that generated in the AD-MEC without biogas circulation based on SEM and XRD analysis (Fig. S7). The current of the AD-MEC with silicates addition was also higher than that without silicates addition (Fig. S8) owing to the improved conductivity. Biogas circulation did not influence the achievement of mineral CO_2 sequestration and nutrients removal in the AD-MEC. However, the pH at the end of each batch with biogas circulation (8.08 ± 0.05) was slightly lower than that without biogas circulation (8.14 ± 0.02 under silicate dosage 1), which may be due to the more dissolved CO_2 under biogas circulation. While the declined pH is not conducive to the formation of struvite, and resulted in the decreased removal of the nutrients under biogas circulation (34.2% for NH_4^+-N and 90.7% for PO_4^{3-}-P) compared to that without biogas circulation (Fig. 2, 47.4% for NH_4^+-N and 92.1% for PO_4^{3-}-P). Correspondingly, the residual Mg^{2+} at the end of each batch under
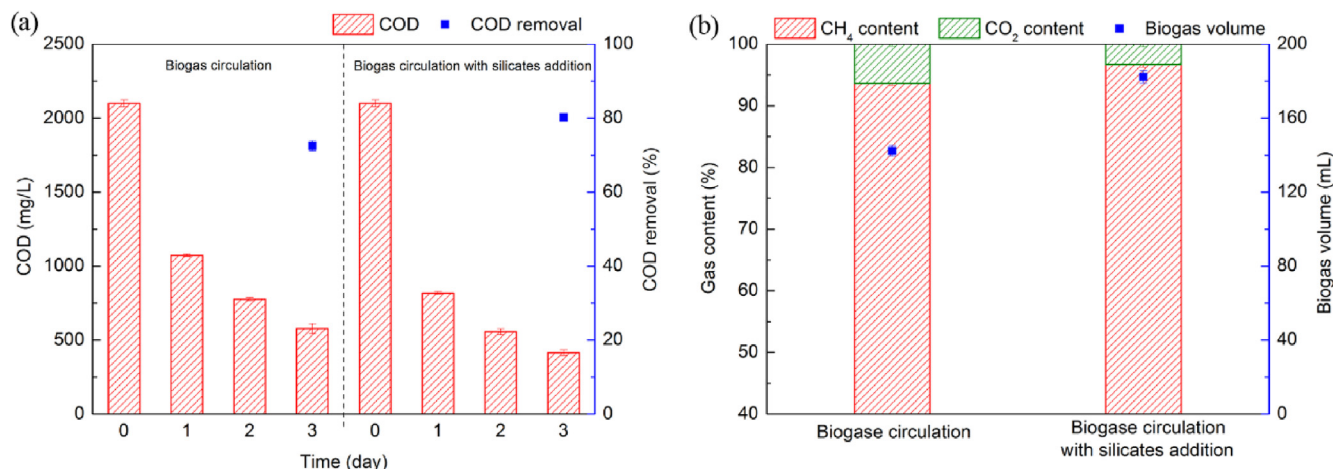

Fig. 4. COD removal and biogas production of the AD-MEC with biogas circulation. (a) COD removal, (b) biogas production. Error bars represent the standard deviations of the four replicate batches under each operation condition.
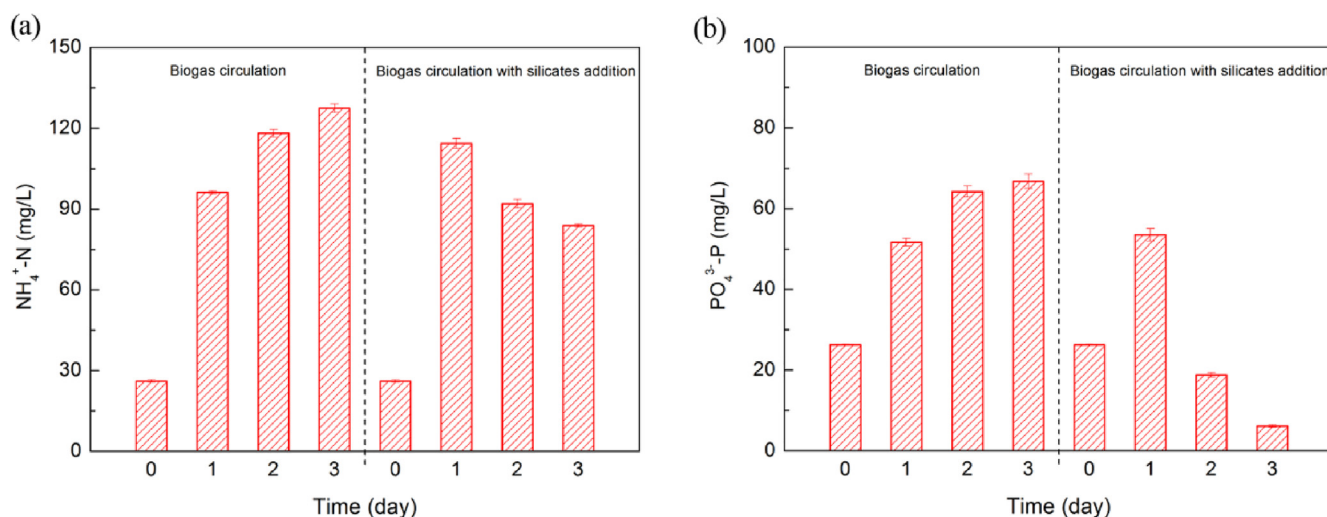
Fig. 5. NH_4^+-N and PO_4^{3-}-P concentrations in the AD-MEC with biogas circulation. (a) NH_4^+-N, (b) PO_4^{3-}-P. Error bars represent the standard deviations of the four replicate batches under each operation condition.

biogas circulation (26.0 ± 0.5 mg/L) was higher than that without biogas circulation under the same silicate dosage (14.0 ± 3.2 mg/L). In addition, the remained Ca^{2+} concentration at the end of each batch under biogas circulation (35.9 ± 0.7 mg/L) was also slightly higher than that without biogas circulation (28.2 ± 2.8 mg/L), which indicated that the amount of CO_2 sequestrated by the formation of calcite might be slightly decreased under biogas circulation, probably owing to the decreased pH. Therefore, compared to the silicates added AD-MEC without biogas circulation, the decreased CO_2 content under biogas circulation was due to the enhanced methanogenesis, not the enhanced mineral CO_2 sequestration. In general, by coupling biogas circulation and silicates application in AD-MEC, the CH_4 content in the biogas was increased from 88.5% ± 0.1% to 96.7% ± 0.4%, with NH_4^+-N and PO_4^{3-}-P decreased by 34.2% and 90.7%, respectively.

This study achieved mineral CO_2 sequestration and nutrients removal in AD-MEC for the first time. CH_4 content was increased from 88.5% ± 0.1% to 92.2% ± 0.2%, with NH_4^+-N and PO_4^{3-}-P decreased by 47.4% and 92.1%, respectively, in the AD-MEC by silicates addition. By integrating with biogas circulation, the CH_4 content could reach 96.7% meeting the requirement of pipeline biomethane [34]. In this case, the biogas upgrading process for CO_2 removal is not required, which would simplify the process, reduce the cost of methane production, and decrease the risk of GHG leakage. The removal of NH_4^+-N (47.4%) was less than that of PO_4^{3-}-P (92.1%), which was owing to the higher concentration of NH_4^+ than PO_4^{3-} in the AD-MEC. As the NH_4^+ and PO_4^{3-} were removed in a fixed ratio by forming struvite, the removal of NH_4^+ was restricted by the concentration of PO_4^{3-}.

Biogas circulation has been tested in several AD systems, and showed different effects on CH_4 production, e.g. CH_4 production rate enhancement [35], CH_4 yield increase [36,37], CH_4 content improvement [38], and some negative effects like CH_4 production decrease [39]. The different effects might be due to the different characteristics of the AD systems, such as substrates, organic loading, HRT, and different biogas circulation parameters, like the circulation rate. In the reported AD-MEC, biogas circulation also increased the CH_4 production [40]. Biogas circulation, on the one hand, utilized the 40 times higher solubility of CO_2 than that of CH_4 to increase CH_4 content by supersaturating CO_2 in the liquor [36,38]. On the other hand, biogas circulation promoted the dissolution and utilization of CO_2, which potentially enhanced hydrogenotrophic methanogens, thus improve CH_4 production and increase CH_4 content [40]. In this study, CH_4 production and CH_4 content were greatly improved with biogas circulation, reflecting the advantage of biogas circulation in AD-MEC. Though biogas circulation slightly deteriorated mineral CO_2 sequestration and

nutrients removal owing to the decreased pH, silicates addition coupled with biogas circulation achieved a very attractive performance in AD-MEC with CH_4 content reached 96.7% ± 0.4%, and NH_4^+-N and PO_4^{3-}-P decreased by 34.2% and 90.7%, respectively.

In this study, the added silicates were filled in a dialysis bag to prevent them from adhering to the electrodes. For practical application in a full-scale plant, the silicates could be filled in filter bags made of polymer fabric with suitable pore size to achieve the same effect. A sequential batch mode was adopted in this study, as it can realize a process of pH decreasing first and increasing subsequently and enhance the release of cations and the sequestration of CO_2 and nutrients. For full-scale plants, the batch operation mode is also preferred. However, continuous flow operation mode should be able to achieve mineral CO_2 and nutrients sequestration as well, as the protons generated by the anode can be used to release cations from silicates and the relatively high pH near the cathode is also conducive to the formation of precipitates. The frequency of silicate replacement should be determined based on the cations inventory remained in the silicates during operation, which may be different under diverse operation conditions. To replace the silicates, the operator only needs to take out the bag containing the silicates and replace the used silicates with an equal amount of new silicates. This is another benefit of holding silicates with a filter bag, in addition to preventing particle from adhering to the electrodes. For decreasing the cost of silicate materials, wastes containing silicates are recommended to be used for mineral CO_2 sequestration and nutrients removal. For example, incineration bottom ash with high calcium silicate content has been applied in AD and successfully achieved CO_2 sequestration [33]. Utilization of silicate contained wastes could significantly reduce the cost and promote the economic viability of mineral CO_2 sequestration and nutrient removal coupled in AD-MEC. The generated precipitates could be separated from the effluent by sedimentation based on its high density. A settling tank is needed following the reactor. The disposal of the precipitates is an issue that needs to be considered. The calcite in the precipitates might be used as building materials, however, the presence of struvite will pose a risk of N and P leakage. The struvite alone can be used as a N and P fertilizer, while calcaite is an unfavorable component accompanied. Therefore, further researches are recommended to investigate the methods for separating the two precipitates from each other, or developing suitable ways of utilization of the combined precipitates. Utilization of generated precipitates, as well as exploring silicates contained waste and enhancing the release of cations from the silicates, are strongly recommended to promote the economic viability of the proposed process.
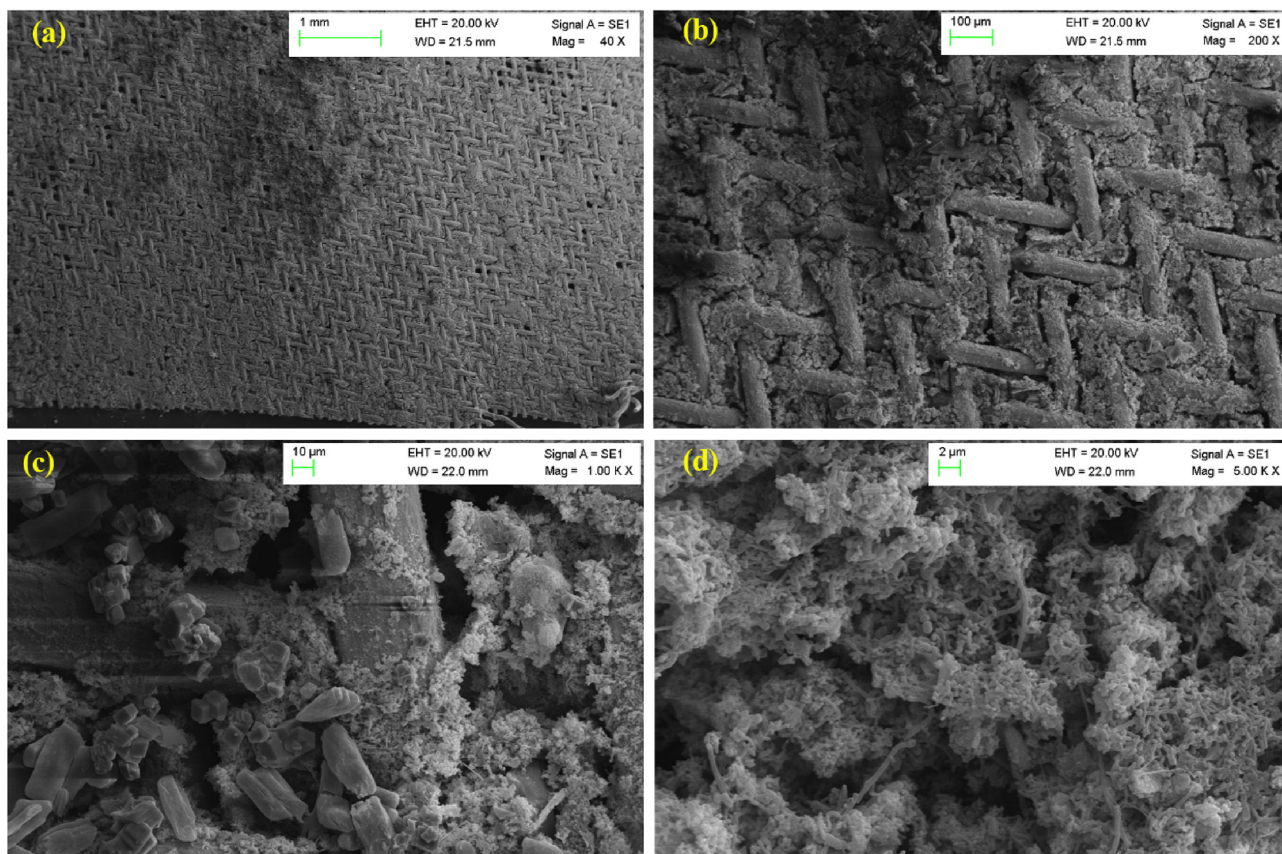
Fig. 6. The morphology of the biocathode in the AD-MEC observed by SEM. (a) 40×, (b) 200×, (c) 1000×, (d) 5000×.

3.3. Microbial community of the AD-MEC with silicate addition

In the process of mineral CO_2 sequestration and nutrients removal in AD-MEC, a potential risk is the accumulation of the generated precipitates on the cathode, as the local pH near the cathode is generally higher than the bulk liquid and benefits for precipitates formation [41–43]. If the precipitates accumulated on the cathode, the long term performance of the process might be deteriorated owing to the influence on biofilm by accumulated precipitates. Therefore, the morphology of the biofilm on cathode was observed based on SEM in this study. In addition, the microbial communities on both electrodes were analyzed. As sampling of biofilm on the electrodes might destroy the bioelectrodes and influence the performance of the reactor, the biofilms on the electrodes were not sampled during the operation, but only sampled at the end of operation. After operation, two small pieces of cathode and anode were cut from the AD-MEC for analysis. The morphology of the cathode biofilm was observed based on SEM. As shown in Fig. 6a, biofilm covered on the 200-mesh nickel cathode without obvious large precipitate particles. Under a magnification of 200 times (Fig. 6b), only a few small precipitate particles were found deposited on the biofilm. The shape of the deposited precipitates (Fig. 6c) was consistent with that collected from the effluent. The small amount of deposit precipitated particles did not significantly affect the biofilm, and the internal structure of the biofilm was still very dense (Fig. 6d). The dense biofilm on the cathode also was the foundation of the excellent performance of the AD-MEC. Since biofilm samples were not collected before biogas circulation, the impact of biogas circulation on the morphology of cathode biofilm can not be accurately evaluated by comparing biofilm samples before and after biogas circulation. However, the dense biofilm and few attached precipitates on the cathode indicated that biogas circulation affects little on the structure of the cathode biofilm.

DNA was extracted from the cathode and anode biofilms to construct bacterial 16S rRNA and archaeal 16S rRNA gene libraries. According to the analysis of the libraries (Table S1), the diversity and richness of the bacterial community (Shannon 3.2458-3.4214, Chao 1 432-467) were significantly higher than that of the archaeal community (Shannon 1.6672-1.8497, Chao 1 19-22). Meanwhile, the diversity and richness of the communities on cathode were slightly higher than that on anode. The dominant classes on the electrodes are shown in Fig. 7. The main bacterial and archaeal classes on cathode and anode were generally the same, with slight differences in relative abundance. The similar microbial communities on the cathode and anode might be because the reactor was a single chamber MEC, and the cathode and anode were started up simultaneously with the same inoculum. Due to the different micro-environments of cathode and anode, although the microbial communities on the two electrodes were similar, the active microorganisms might be different.

For the bacterial community, Deltaproteobacteria, Clostridia, Bacteroidia, Ignavibacteria, and norank_p_WS6 were the main classes. On the anode, Deltaproteobacteria dominated with a relative abundance of 29.8%, while the other four classes were with similar relative abundance of 10.7%–12.2%. On the cathode, Clostridia was the most dominant class with relative abundance of 22.8%, Deltaproteobacteria was slightly lower (20.0%), while the other three classes were at 7.2%–12.9%. Deltaproteobacteria is a genus with diverse functions widely distributed in various natural environments [44,45], and engineering reactors [46] including anaerobic digestion [47] and bioelectrochemical reactor [48]. Ignavibacteria is a bacterial class that has been found in anaerobic reactor treating organic wastewater, which increased from less than 1% to 54.0% when the reactor switched from aerobic to anaerobic operation [49]. Clostridia and Bacteroidia are key acidification members responsible for VFAs/H_2 production [50]. The main bacterial composition was consistent with the relatively high
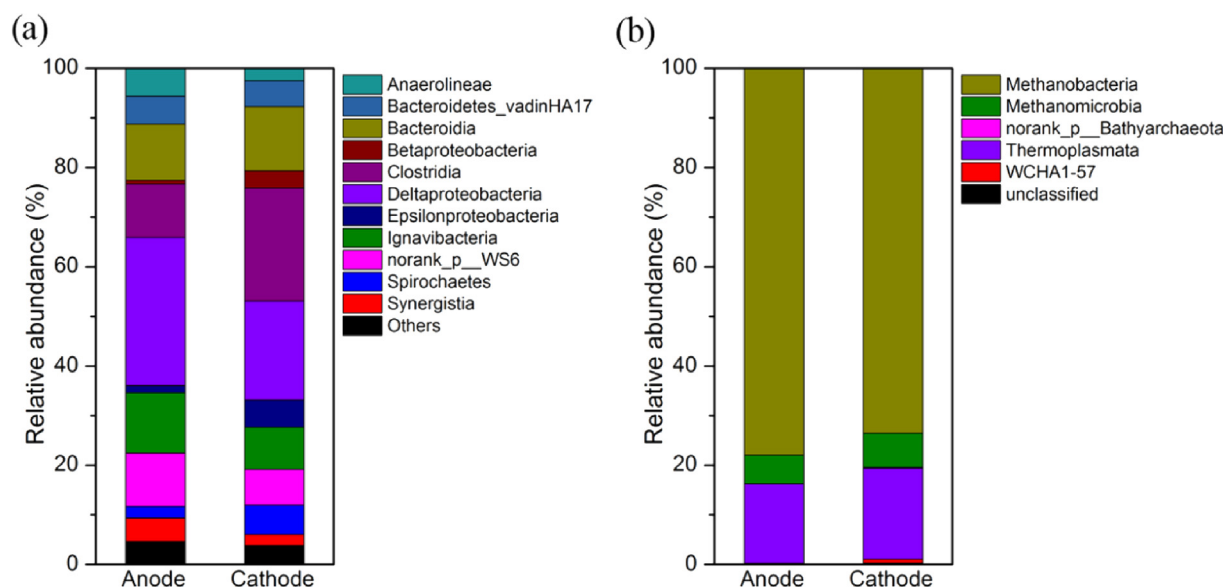
Fig. 7. Dominant classes of the microbial communities on the electrodes. (a) Bacterial classes, the classes with abundance < 1% were assigned into "Others"; (b) archaeal classes, sequences that could not be classified into a known group were assigned into "Unclassified". "Anode" means the sample collected from the anode of the AD-MEC at the end of operation; "Cathode" means the sample collected from the cathode of the AD-MEC at the end of operation.
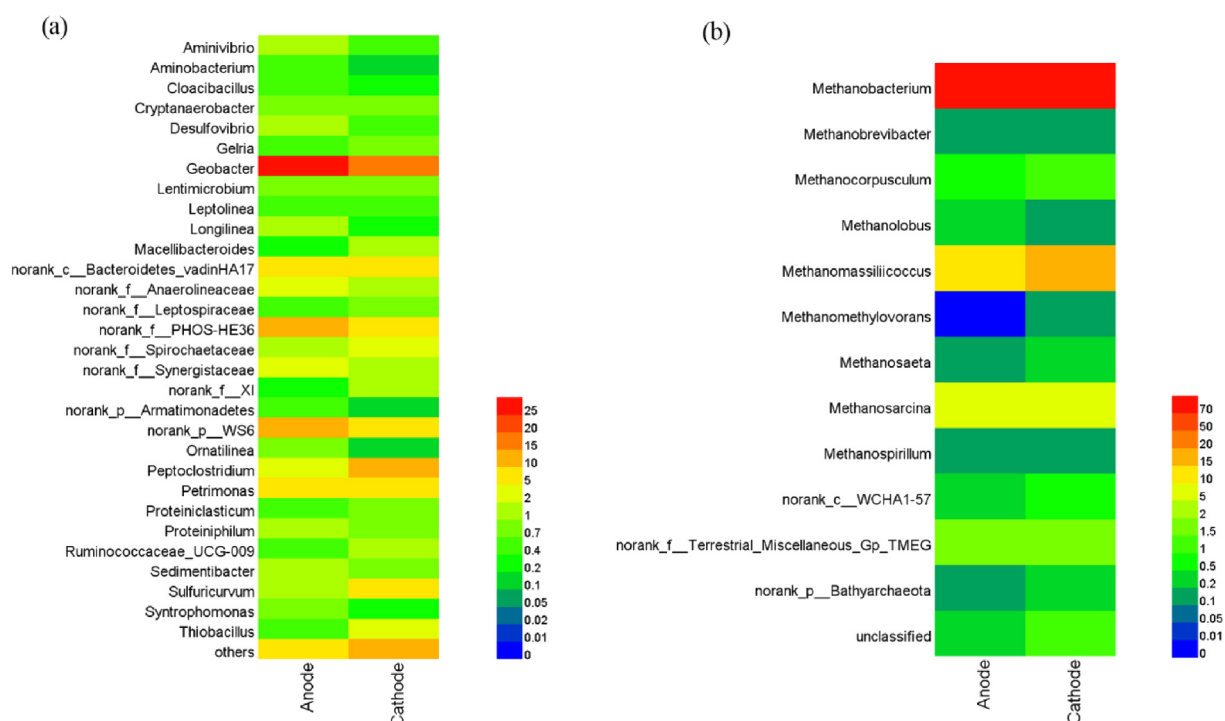
Fig. 8. Relative abundances of main genera (abundance > 1%) in the microbial communities on the electrodes. (a) Bacterial genera; (b) archaeal genera. "Anode" means the sample collected from the anode of the AD-MEC at the end of operation; "Cathode" means the sample collected from the cathode of the AD-MEC at the end of operation.

organic removal of the AD-MEC. On the genus level, *Geobacter* was the dominant bacterial genus with relative abundance of 16.1% on cathode and 27.0% on anode (Fig. 8a). In addition, norank_f_PHOS-HE36 and norank_p_WS6, with relative abundance of 12.2% and 10.8%, respectively, were other two main genera. While *Peptoclostridium* with a relative abundance of 13.5% inhabited on the cathode. *Geobacter* is a group of typical electroactive microorganisms with both outward and inward extracellular electron transfer ability [51,52], which usually enriched on anode higher than on cathode [53,54], and potentially played a key role in electron transfer in MEC.

For archaeal communities, Methanobacteria with a relative abundance of 73.5%–78.0% was the dominant class on both cathode and anode (Fig. 7b). Thermoplasmata with a relative abundance of 15.9%–18.4% was higher than that of Methanomicrobia (5.8%–6.9%). Other archaeal classes accounted for very low relative abundances. Methanobacteria and Methanomicrobia are two methanogen groups commonly found in ADs and AD-MECs [12,55,56], while Thermoplasmata is a distinct group rather than methanogens which is not ubiquitous in ADs [57]. On the genus level, *Methanobacterium* was the dominant archaeal genus with relative abundance of 77.7% on anode

and 72.6% on cathode (Fig. 8b). *Methanomassiliicoccus* with relative abundance of 14.2% and 16.7% on anode and cathode, respectively, was another main archaeal genus in the AD-MEC. Both *Methanobacterium* and *Methanomassiliicoccus* are typical hydrogenotrophic methanogens [57–59]. On the contrary, *Methanosarcina*, the facultative acetoclastic methanogen [59,60], only accounted for 5.1% and 5.7% on anode and cathode, respectively. The overwhelming relative abundance of hydrogenotrophic methanogens indicated that the hydrogenotrophic methanogenesis was the dominant methanogenesis pathway for methane production. The dominant hydrogenotrophic methanogens in the archaeal community together with the abundant electroactive *Geobacter* and organic matter degrading microorganisms resulted in the high CH_4 production and CH_4 content of the AD-MEC with silicates addition and biogas circulation.

4. Conclusion

This study, for the first time, achieved mineral CO_2 sequestration and nutrients removal in AD-MEC with wollastonite and magnesium silicate addition. Keeping wollastonite and magnesium silicate in the ratio for almost equal Ca^{2+} and Mg^{2+} release, increase the dosage of silicates addition enhanced the performance of CO_2 sequestration and nutrients removal before reaching proton inventory. Under optimal dosage of 20 g/L wollastonite and 40 g/L magnesium silicate, NH_4^+ and PO_4^{3-} was removed by 47.4% and 92.1%, respectively, with CO_2 content decreased from 11.5% to 7.8%. Biogas circulation slightly deteriorated mineral CO_2 sequestration and nutrients removal in AD-MEC, but enhanced CH_4 production from 164.8 mL CH_4/g CODr to 261.5 $\pm$ 5.1 mL CH_4/g CODr. Integrating biogas circulation with silicates application in AD-MEC increased CH_4 content to 96.7% $\pm$ 0.4%. Calcite and struvite precipitates generated in the AD-MEC with mineral CO_2 sequestration and nutrients removal. *Geobacter* was the dominant bacterial genus on both anode and cathode, while hydrogenotrophic methanogens *Methanobacterium* and *Methanomassiliicoccus* dominated in archaeal communities on the electrodes. In conclusion, the combined application of wollastonite and magnesium silicate is an attractive way to improve the performance of AD-MEC by achieving CO_2 sequestration and nutrients removal.

Declaration of Competing Interest

The authors declare that they have no known competing financial interests or personal relationships that could have appeared to influence the work reported in this paper.

Acknowledgements

Appendix A. Supplementary data

Supplementary data to this article can be found online at https://doi.org/10.1016/j.cej.2020.125680.

References

[1] M.B. Shahabadi, L. Yerushalmi, F. Haghighat, Impact of process design on greenhouse gas (GHG) generation by wastewater treatment plants, Water Res. 43 (2009) 2679–2687.

[2] H. Yoshida, J. Monster, C. Scheutz, Plant-integrated measurement of greenhouse gas emissions from a municipal wastewater treatment plant, Water Res. 61 (2014) 108–118.

[3] W. Hu, J. Tian, L. Chen, Greenhouse gas emission by centralized wastewater treatment plants in Chinese industrial parks: Inventory and mitigation measures, J. Clean Prod. 225 (2019) 883–897.

[4] H. Wang, Y. Yang, A.A. Keller, X. Li, S. Feng, Y.-N. Dong, F. Li, Comparative analysis of energy intensity and carbon emissions in wastewater treatment in USA, Germany, China and South Africa, Appl. Energy 184 (2016) 873–881.

[5] Y. Gu, Y. Li, X. Li, P. Luo, H. Wang, Z.P. Robinson, X. Wang, J. Wu, F. Li, The feasibility and challenges of energy self-sufficient wastewater treatment plants, Appl. Energy 204 (2017) 1463–1475.

[6] P. Jenicek, J. Bartacek, J. Kutil, J. Zabranska, M. Dohanyos, Potentials and limits of anaerobic digestion of sewage sludge: Energy self-sufficient municipal wastewater treatment plant? Water Sci. Technol. 66 (2012) 1277–1281.

[7] I. Angelidaki, L. Treu, P. Tsapekos, G. Luo, S. Campanaro, H. Wenzel, P.G. Kougias, Biogas upgrading and utilization: Current status and perspectives, Biotechnol. Adv. 36 (2018) 452–466.

[8] Y. Li, Y. Chen, J. Wu, Enhancement of methane production in anaerobic digestion process: A review, Appl. Energy 240 (2019) 120–137.

[9] Z.S. Yu, X.Y. Leng, S. Zhao, J. Ji, T.Y. Zhou, A. Khan, A. Kakde, P. Liu, X.K. Li, A review on the applications of microbial electrolysis cells in anaerobic digestion, Bioresour. Technol. 255 (2018) 340–348.

[10] Z. Dou, C.M. Dykstra, S.G. Pavlostathis, Bioelectrochemically assisted anaerobic digestion system for biogas upgrading and enhanced methane production, Sci. Total Environ. 633 (2018) 1012–1021.

[11] A. Hassanein, F. Witarsa, X.H. Guo, L. Yong, S. Lansing, L. Qiu, Next generation digestion: Complementing anaerobic digestion (AD) with a novel microbial electrolysis cell (MEC) design, Int. J. Hydrogen Energy 42 (2017) 28681–28689.

[12] B. Lee, J.G. Park, W.B. Shin, D.J. Tian, H.B. Jun, Microbial communities change in an anaerobic digestion after application of microbial electrolysis cells, Bioresour. Technol. 234 (2017) 273–280.

[13] J. Park, B. Lee, D. Tian, H. Jun, Bioelectrochemical enhancement of methane production from highly concentrated food waste in a combined anaerobic digester and microbial electrolysis cell, Bioresour. Technol. 247 (2018) 226–233.

[14] J.L. Linville, Y. Shen, M. Urgun-Demirtas, S.W. Snyder, Effect of particle size and doses of olivine addition on carbon dioxide sequestration during anaerobic digestion of sewage sludge at ambient and mesophilic temperatures, Process Biochem. 51 (2016) 59–72.

[15] J.L. Linville, Y. Shen, R.P. Schoene, M. Nguyen, M. Urgun-Demirtas, S.W. Snyder, Impact of trace element additives on anaerobic digestion of sewage sludge with in-situ carbon dioxide sequestration, Process Biochem. 51 (2016) 1283–1289.

[16] W. Seifritz, CO_2 disposal by means of silicates, Nature 345 (1990) 486.

[17] S.S. Salek, R. Kleerebezem, H.M. Jonkers, G.-J. Witkamp, M.C.M. van Loosdrecht, Mineral CO_2 sequestration by environmental biotechnological processes, Trends Biotechnol. 31 (2013) 139–146.

[18] H. Liu, L. Gong, Y. Zhang, Q. Jiang, M. Cui, J. Zhang, B. Fu, H. Liu, Silicate mediated simultaneous in-situ CO_2 sequestration and nutrients removal in anaerobic digestion, Bioresour. Technol. 282 (2019) 125–132.

[19] Y. Zhang, L. Zhang, H. Liu, L. Gong, Q. Jiang, H. Liu, B. Fu, Carbon dioxide sequestration and methane production promotion by wollastonite in sludge anaerobic digestion, Bioresour. Technol. 272 (2018) 194–201.

[20] State Environmental Protection Administration of China, Standard Methods for the Analysis of Water and Wastewater, China Environmental Science Publishing House, Beijing, 2002.

[21] F. Abouelenien, Y. Kitamura, N. Nishio, Y. Nakashimada, Dry anaerobic ammonia-methane production from chicken manure, Appl. Microbiol. Biot. 82 (2009) 757–764.

[22] T. Dai, Y. Zhang, Y. Tang, Y. Bai, Y. Tao, B. Huang, D. Wen, Identifying the key taxonomic categories that characterize microbial community diversity using full-scale classification: a case study of microbial communities in the sediments of Hangzhou Bay, Fems, Microbiol. Ecol. 93 (2017) fiw203.

[23] R.C. Edgar, Search and clustering orders of magnitude faster than BLAST, Bioinformatics 26 (2010) 2460–2461.

[24] C. Quast, E. Pruesse, P. Yilmaz, J. Gerken, T. Schweer, P. Yarza, J. Peplies, F.O. Gloeckner, The SILVA ribosomal RNA gene database project: improved data processing and web-based tools, Nucleic Acids Res. 41 (2013) D590–D596.

[25] J.R. Cole, Q. Wang, E. Cardenas, J. Fish, B. Chai, R.J. Farris, A.S. Kulam-Syed-Mohideen, D.M. McGarrell, T. Marsh, G.M. Garrity, J.M. Tiedje, The Ribosomal Database Project: improved alignments and new tools for rRNA analysis, Nucleic Acids Res. 37 (2009) D141–D145.

[26] K. Hu, L. Xu, W. Chen, S.Q. Jia, W. Wang, F. Han, Degradation of organics extracted from dewatered sludge by alkaline pretreatment in microbial electrolysis cell, Environ. Sci. Pollut. Res. 25 (2018) 8715–8724.

[27] R.E.F. Lindeboom, I. Ferrer, J. Weijma, J.B. van Lier, Silicate minerals for CO_2 scavenging from biogas in Autogenerative High Pressure Digestion, Water Res. 47 (2013) 3742–3751.

[28] P. d'Abzac, F. Bordas, E. Joussein, E. van Hullebusch, P.N.L. Lens, G. Guibaud, Characterization of the mineral fraction associated to extracellular polymeric substances (EPS) in anaerobic granular sludges, Environ. Sci. Technol. 44 (2010) 412–418.

[29] H. Liu, J. Wang, X. Liu, B. Fu, J. Chen, H-Q. Yu, Acidogenic fermentation of proteinaceous sewage sludge: Effect of pH, Water Res. 46 (2012) 799–807.

[30] H. Ma, X. Chen, H. Liu, H. Liu, B. Fu, Improved volatile fatty acids anaerobic production from waste activated sludge by pH regulation: Alkaline or neutral pH? Waste Manage. 48 (2016) 397–403.

[31] Y. Dang, R. Zhang, S. Wu, Z. Liu, B. Qiu, Y. Fang, D. Sun, Calcium effect on

anaerobic biological treatment of fresh leachate with extreme high calcium concentration, Int. Biodeter. Biodegr. 95 (2014) 76–83.

[32] S. Kumar, A. Das, G.L.K. Srinivas, H. Dhar, V.K. Ojha, J. Wong, Effect of calcium chloride on abating inhibition due to volatile fatty acids during the start-up period in anaerobic digestion of municipal solid waste, Environ. Technol. 37 (2016) 1501–1509.

[33] C. Yin, Y. Shen, N. Zhu, Q. Huang, Z. Lou, H. Yuan, Anaerobic digestion of waste activated sludge with incineration bottom ash: Enhanced methane production and CO_2 sequestration, Appl. Energy 215 (2018) 503–511.

[34] Y. Shen, J.L. Linville, M. Urgun-Demirtas, R.P. Schoene, S.W. Snyder, Producing pipeline-quality biomethane via anaerobic digestion of sludge amended with corn stover biochar with in-situ CO_2 removal, Appl. Energy 158 (2015) 300–309.

[35] S.R. Lee, N.K. Cho, W.J. Maeng, Using the pressure of biogas created during anaerobic-digestion as the source of mixing power, J. Ferment. Bioeng. 80 (1995) 415–417.

[36] K. Latha, R. Velraj, P. Shanmugam, S. Sivanesan, Mixing strategies of high solids anaerobic co-digestion using food waste with sewage sludge for enhanced biogas production, J. Clean Prod. 210 (2019) 388–400.

[37] N.I. Siddique, M.S.A. Munaim, Z.A. Wahid, Role of biogas recirculation in enhancing petrochemical wastewater treatment efficiency of continuous stirred tank reactor, J. Clean Prod. 91 (2015) 229–234.

[38] T. Yuan, Y.F. Cheng, X.Z. Wang, Y. Yu, Z.Y. Zhang, Z.F. Lei, K. Shimizu, M. Utsumi, Y. Adachi, D.J. Lee, A novel anaerobic digestion system coupling biogas recirculation with $MgCl_2$ addition for multipurpose sewage sludge treatment, J. Clean Prod. 230 (2019) 499–507.

[39] K. Karim, K.T. Klasson, R. Hoffmann, S.R. Drescher, D.W. DePaoli, M.H. Al-Dahhan, Anaerobic digestion of animal waste: Effect of mixing, Bioresour. Technol. 96 (2005) 1607–1612.

[40] K. Yanuka-Golub, K. Baransi-Karkaby, A. Szczupak, L. Reshef, J. Rishpon, R. Shechter, U. Gophna, I. Sabbah, An electrode-assisted anaerobic digestion process for the production of high-quality biogas, Water Sci. Technol. 79 (2019) 2145–2155.

[41] R.D. Cusick, M.L. Ullery, B.A. Dempsey, B.E. Logan, Electrochemical struvite precipitation from digestate with a fluidized bed cathode microbial electrolysis cell, Water Res. 54 (2014) 297–306.

[42] T.P. Sciarria, G. Vacca, F. Tambone, L. Trombino, F. Adani, Nutrient recovery and energy production from digestate using microbial electrochemical technologies (METs), J. Clean Prod. 208 (2019) 1022–1029.

[43] P.Y. Yuan, Y. Kim, Increasing phosphorus recovery from dewatering centrate in microbial electrolysis cells, Biotechnol. Biofuels 10 (2017) 70.

[44] A. Robador, A.L. Mueller, J.E. Sawicka, D. Berry, C.R.J. Hubert, A. Loy, B.B. Jorgensen, V. Bruchert, Activity and community structures of sulfate-reducing microorganisms in polar, temperate and tropical marine sediments, ISME J. 10 (2016) 796–809.

[45] Y. Zhang, L. Chen, R. Sun, T. Dai, J. Tian, W. Zheng, D. Wen, Temporal and spatial changes of microbial community in an industrial effluent receiving area in Hangzhou Bay, J. Environ. Sci. 44 (2016) 57–68.

[46] Y. Zhang, L. Chen, R. Sun, T. Dai, J. Tian, R. Liu, D. Wen, Effect of wastewater disposal on the bacterial and archaeal community of sea sediment in an industrial

area in China, FEMS Microbiol. Ecol. 88 (2014) 320–332.

[47] M. Fujimoto, D.E. Carey, D.H. Zitomer, P.J. McNamara, Syntroph diversity and abundance in anaerobic digestion revealed through a comparative core microbiome approach, Appl. Microbiol. Biot. 103 (2019) 6353–6367.

[48] J. Wang, X. Song, Q. Li, H. Bai, C. Zhu, B. Weng, D. Yan, J. Bai, Bioenergy generation and degradation pathway of phenanthrene and anthracene in a constructed wetland-microbial fuel cell with an anode amended with nZVI, Water Res. 150 (2019) 340–348.

[49] J. Zhu, L. Chen, Y. Zhang, X. Zhu, Revealing the anaerobic acclimation of microbial community in a membrane bioreactor for coking wastewater treatment by Illumina Miseq sequencing, J. Environ. Sci. 64 (2018) 139–148.

[50] W. Huang, F. Yang, W. Huang, Z. Lei, Z. Zhang, Enhancing hydrogenotrophic activities by zero-valent iron addition as an effective method to improve sulfadiazine removal during anaerobic digestion of swine manure, Bioresour. Technol. 294 (2019) 122178.

[51] Y. Jiang, R.J. Zeng, Bidirectional extracellular electron transfers of electrode-biofilm: Mechanism and application, Bioresour. Technol. 271 (2019) 439–448.

[52] B.E. Logan, R. Rossi, A.A. Ragab, P.E. Saikaly, Electroactive microorganisms in bioelectrochemical systems, Nat. Rev. Microbiol. 17 (2019) 307–319.

[53] C. Lin, P. Wu, Y. Liu, J.W.C. Wong, X. Yong, X. Wu, X. Xie, H. Jia, J. Zhou, Enhanced biogas production and biodegradation of phenanthrene in wastewater sludge treated anaerobic digestion reactors fitted with a bioelectrode system, Chem. Eng. J. 365 (2019) 1–9.

[54] B.S. Zakaria, L. Lin, B.R. Dhar, Shift of biofilm and suspended bacterial communities with changes in anode potential in a microbial electrolysis cell treating primary sludge, Sci. Total Environ. 689 (2019) 691–699.

[55] W. Cai, W. Liu, Z. Zhang, K. Feng, G. Ren, C. Pu, J. Li, Y. Deng, A. Wang, Electro-driven methanogenic microbial community diversity and variability in the electron abundant niche, Sci. Total Environ. 661 (2019) 178–186.

[56] J. Zhao, Y. Li, S. Pan, Q. Tu, W. Dang, Z. Wang, H. Zhu, Effects of magnesium chloride on the anaerobic digestion and the implication on forward osmosis membrane bioreactor for sludge anaerobic digestion, Bioresour. Technol. 268 (2018) 700–707.

[57] B. Dridi, M.-L. Fardeau, B. Ollivier, D. Raoult, M. Drancourt, Methanomassiliicoccus luminyensis gen. nov., sp nov., a methanogenic archaeon isolated from human faeces, Int. J. Syst. Evol. Micr. 62 (2012) 1902–1907.

[58] K. Lang, J. Schuldes, A. Klingl, A. Poehlein, R. Daniel, A. Brune, New mode of energy metabolism in the seventh order of methanogens as revealed by comparative genome analysis of "Candidatus Methanoplasma termitum", Appl. Environ. Microb. 81 (2015) 1338–1352.

[59] Z. Yang, W. Wang, C. Liu, R. Zhang, G. Liu, Mitigation of ammonia inhibition through bioaugmentation with different microorganisms during anaerobic digestion: selection of strains and reactor performance evaluation, Water Res. 155 (2019) 214–224.

[60] L. Hao, F. Lue, L. Mazeas, E.D.-L. Quemener, C. Madigou, A. Guenne, L. Shao, T. Bouchez, P. He, Stable isotope probing of acetate fed anaerobic batch incubations shows a partial resistance of acetoclastic methanogenesis catalyzed by Methanosarcina to sudden increase of ammonia level, Water Res. 69 (2015) 90–99.